

Improvement of Sinter Productivity by Adding Return Fine on Raw Materials after Granulation Stage (Development of RF-MEBIOS)

Masaru MATSUMURA* Yasuhide YAMAGUCHI
Chikashi KAMIJO

Abstract

In order to increase the permeability of the sintering bed for sinter ore productivity, the RF-MEBIOS (Return Fine - Mosaic Embedding Iron Ore Sintering) process, in which return fine as dry particle is added to granulated raw materials and then charged into the sintering machine, is proposed. This productivity increase is caused by increasing the pseudo-particle size at granulation and by decreasing the bulk density of the sinter packed bed after charging. The former is achieved by a higher moisture content in the raw materials at granulation. The latter is achieved by higher friction in the sintering bed composed of a dry and wet particle compound, which has a role of decreasing bulk density. Based on the sintering pot test, by increasing the bypass return fine ratio and size, the sintering speed and sinter productivity increased. In addition, the effect of pseudo-particle size and bulk density on flame front speed were evaluated as 55% and 41%, respectively.

1. Introduction

Sinter productivity strongly depends on the sinter permeability of a sinter packed bed. This is because the faster the progress of reaction sintering, the higher the flow rate of the gas passing the sinter packed bed and the gas flow rate is controlled by the sinter permeability. Furthermore, high sinter permeability is achieved by larger pseudo-particles, which are sinter raw materials after granulation, and a higher void ratio of sinter packed beds represented as the Ergun Formula.

In fact, charging mini-pellets,^{1,2)} which are large particles as pseudo-particles in the sinter process, has a role of increasing permeability. To increase the pseudo-particle size, a separate granulation process is effective.³⁾ The separate granulation process has two or more granulation routes. This process has been applied in many sinter plants in Japan⁴⁻⁶⁾ based on fundamental study as duplex mini-pellets.⁷⁾ When introducing the process, granulation devices generally called “mixers” have also been examined to determine essential mechanical parameters, such as the angle size and rotation speed.⁸⁾

On the other hand, a high void ratio of sinter packed beds that is

the other capital parameter for high permeability has been mainly achieved by a charging apparatus for loose packing. In addition to the high void ratio at charging, maintaining the high void ratio during sintering is necessary. An effective solution is decreasing the moisture content in granulated sinter raw materials while maintaining the pseudo-particle size⁹⁾ to reduce the quantity of condensed water in the sintering process¹⁰⁾ as a method to maintain the void ratio from the perspective of water behavior in sinter packed beds, in addition to enhancement of the pseudo-particle strength by blending more quick lime.¹¹⁾ This is because water that functions as a binder in granulation hinders the ventilation during sintering.

Recently, as a technology for improving the permeability of sintered packed beds focusing on the pseudo-particle size and the void ratio, Mosaic Embedding Iron Ore Sintering (MEBIOS)¹²⁻¹⁵⁾ has been proposed. **Figure 1**^{12,15)} illustrates the sintering bed structure of the MEBIOS process. The MEBIOS process can be used to obtain a high density, high permeability packed bed by setting denser parts with a low density in the same packed bed. For example, high-density large green balls with a diameter of 5 to 15 mm are placed

* Chief Researcher, Ph.D.(Environmental studies), Ironmaking Research Lab., Process Research Laboratories
20-1 Shintomi, Futtsu City, Chiba Pref. 293-8511

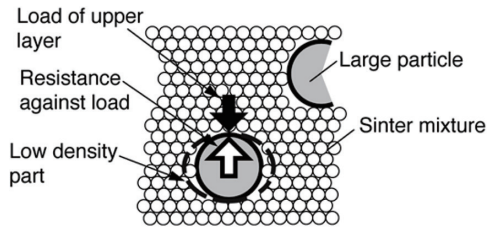


Fig. 1 Denser parts and loser ones in the same packed bed of MEBIOS^{12, 15)}

in a packed bed to create lower density parts (voids) around the balls by a wall effect, so that the permeability of the entire packed bed increases. It has been confirmed that MEBIOS also has a role of maintaining a high void ratio during sintering because during the sintering, large dense particles can maintain their shape and partially aggregate with the surrounding loose packed parts in the sinter packed bed.^{16, 17)}

In recent years, technologies to apply MEBIOS with a low capital investment have been studied. It has been confirmed that even small dry particles charged into a sinter packed bed have a similar effect to that of high-density large green balls on controlling the bed structure with the friction between dry particles and granulated wet pseudo-particles. In charging a sinter mixture into a sinter plant, the friction acting between the dry and wet particles can suppress them from being densely packed, which can maintain the high void ratio. In addition, the moisture content can be individually controlled in granulation and charging into the sintering bed. Specifically, the high moisture content in the granulation stage can accelerate the granulation, and then add dry particles to form a sintering packed bed with a low moisture content in charging. For a practical sinter plant, return fines are used as dry particles by bypassing the mixing and granulating routes. This process is called Return Fine - Mosaic Embedding Iron Ore Sintering (RF-MEBIOS). The return fines can be used as the dry particles by eliminating the drying process because the return fines are utilized as raw materials soon after they are discharged from sinter plants.

In this report, from the viewpoint of the bulk density in sinter packed beds and the pseudo-particle size after mixing and granulation, permeability improvement techniques based on RF-MEBIOS were studied by a pot test. Thereafter, the process was applied to sinter plants to improve the productivity in each sinter plant. RF-MEBIOS can be used for not only improving the sinter productivity, but also countermeasures against the recent increase in the amount of fine ore.³⁾

2. Sinter Pot Examination

2.1 Experimental procedures

The effect of the RF-MEBIOS process on the sinter productivity was evaluated in a pot test. Figure 2 shows the experimental flow of the pot test. At first, 85 mass% of the total raw materials, which were several types of fine ore, serpentine, and limestone, and 15 mass% of the return fines were prepared. Detailed blending conditions are shown in Table 1. Some of the return fines ($x\%$) were added into the granulated sinter raw materials and the remaining return fines ($15-x\%$) were used for the granulation. The former are called bypass return fines and the latter are granulation return fines.

Then, the raw materials except the bypass return fines were mixed in a drum-type mixer (diameter: 600 mm, length: 800 mm) for 4 min, and a designated amount of water was sprayed and mixed again for 4 min. The mixing after the water spraying causes granulation. Then, the bypass return fines were mixed into the granulated raw material for 15 s. This was used as the blending material. The moisture content to be added was adjusted such that the moisture content after the bypass return fines were added (hereinafter referred to as a “moisture content at charging”) was 7.0% equally in all cases. Therefore, the higher the percentage of the bypass return fines, the higher the moisture content in the granulation (hereinafter referred to as a “moisture content after granulation”). In this paper, the moisture content (mass%) before the bypass return fines are added is referred to as the “moisture content after granulation” and the moisture content (mass%) after the bypass return fines are added is referred to as the “moisture content at charging”. The former parameter affects granulation and the latter affects sintering. Regarding charging into a pot, 2.0 kg of sinter ore with 10 to 15 mm was placed in a sinter pot (300 mm in diameter \times 500 mm in height) as the hearth material. The sinter raw material was dropped from a height of 680 mm from the hearth material.

Figure 3 shows the influence of the bypass return fine ratio on the moisture contents after the granulation and at charging. The curved line that indicates the designed values matches the marks that indicate the measured values, which means that the expected test results were obtained. The pseudo-particle size was measured both after the granulation and at charging. As the measuring method, a mechanical sieving process using several sizes of mesh was used for 15 s without tapping after dry treatment for 2 h at 105 degrees C.

Table 1 shows the blending conditions. Five main types of iron ore used in Japan were used. The coke breeze blending ratio was set to 4.5% relative to the total sinter mixture. The purpose of Series 1 and Series 2 is to investigate the effects of the bypass return fine ratio and size, respectively. In Series 2, the blending ratios of return fines in +1 mm and -1 mm, which were 7.7% and 7.3% respectively, correspond to the size distribution of the return fines with the -1 mm ratio of 49% shown in Fig. 4.

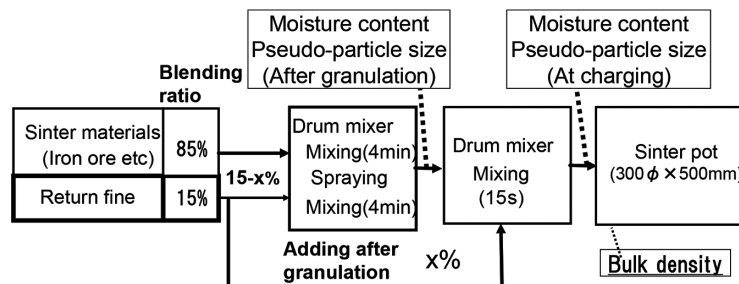


Fig. 2 Experimental flow of pot test (300 mm ϕ)

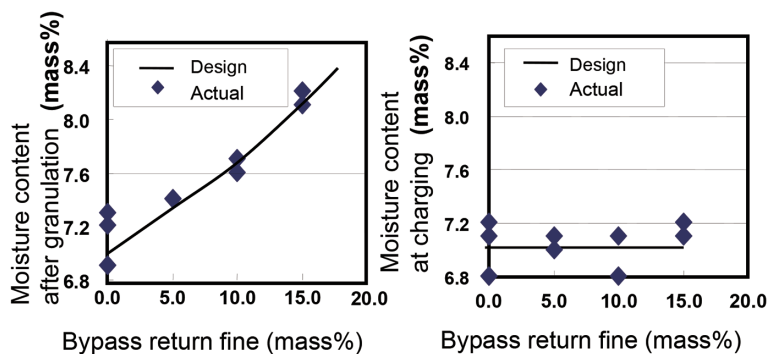


Fig. 3 Moisture content in sinter raw materials after granulation and at charging

Table 1 Blending conditions of sinter mixture

Route	Raw materials	Series 1				Series 2	
Ordinary route	Iron ore R	8.5	8.5	8.5	8.5	8.5	8.5
	Iron ore Y	19.1	19.1	19.1	19.1	19.1	19.1
	Iron ore H	13.2	13.2	13.2	13.2	13.2	13.2
	Iron ore C	8.5	8.5	8.5	8.5	8.5	8.5
	Iron ore W	21.3	21.3	21.3	21.3	21.3	21.3
	Serpentine	2.1	2.1	2.1	2.1	2.1	2.1
	Lime stone	12.3	12.3	12.3	12.3	12.3	12.3
	Return fine	<u>15</u>	<u>10</u>	<u>5</u>	<u>0</u>	-	-
	Return fine (+1 mm)	-	-	-	-	-	<u>7.7</u>
	Return fine (-1 mm)	-	-	-	-	<u>7.3</u>	-
	Sub total	100	95	90	85	92.3	92.7
	Coke breeze (-5 mm)	[4.5]	[4.5]	[4.5]	[4.5]	[4.5]	[4.5]
<u>Added after granulation stage</u>	Return fine	<u>0</u>	<u>5</u>	<u>10</u>	<u>15</u>	-	-
	Return fine (+1 mm)	-	-	-	-	<u>7.7</u>	-
	Return fine (-1 mm)	-	-	-	-	-	<u>7.3</u>
	Sub total	<u>0</u>	<u>5</u>	<u>10</u>	<u>15</u>	<u>7.7</u>	<u>7.3</u>
Total		100	100	100	100	100	100
	Coke breeze (-5 mm)	[4.5]	[4.5]	[4.5]	[4.5]	[4.5]	[4.5]

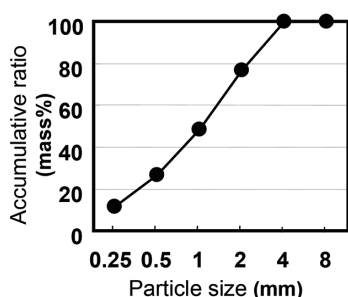


Fig. 4 Size distribution of return fine

Sintering was performed in a window box at a constant pressure of 10.3 kPa, after igniting by an LPG burner for 1 min during suction at 5.2 kPa. The pressure in the window box was controlled by the opening degree of a damper at the main exhaust pipe set between the wind box and a fan. The exhaust gas temperature was measured with a thermocouple installed at the center of the wind box. Sintering was terminated 3 min after the BTP, which is the time point at which the maximum temperature of exhaust gas is measured. The combustion time was defined as the time from the ignition

start to the maximum exhaust gas temperature.

Then sinter cake discharged from the pot was dropped from a height of 2.0 m 4 times after weight measurement. After the drop, it was sieved by 5 mm and the weight (+5 mm) was measured. The weight of the sinter product was determined as the weight of +5-mm particles minus 2.0 kg (hearth material) on the assumption that the powdered hearth material particles smaller than 5 mm have been removed. Then, the yield was obtained by dividing the weight of the sinter product by the weight of the sinter cake minus 2.0 kg. The sinter productivity was calculated by dividing the sinter product weight by the sintering time and the area of the sinter pot.

The frame front speed (FFS) was calculated by dividing the height of the sinter packed bed at charging into the pot by the time from the ignition start to when the burning zone reaches the lowest area of the sinter raw material. The time at which the burning zone reaches the lowest area was set as the rise time of the exhaust gas temperature.

2.2 Results

Figures 5–7 show the results for the productivity, the FFS, and the yield, respectively. With the increase of the ratio of the bypass return fines, the productivity and FFS increased. When the bypass

return fine ratios of 5% and 10% are compared, both have the same level of FFS. Although the reason is not clear, the bypass return fine size distribution remains invariant and, as the bypass return fine ratio is higher, the moisture content in the granulated material monotonously increases. Therefore, it is unlikely that a specific phenomenon occurs in the bypass return fine ratios from 5 to 10%. Accordingly, it is understood that as the bypass return fine ratio increases from 0 to 15%, the FFS monotonously increases.

Bypassing large particles (+1 mm) has better productivity and FFS than the bypassing small particles (-1 mm). In the case of the bypass return fine ratio of 15% (to the total mixture), the pot yield is low, which may be caused by high FFS.

Figure 8 shows the results of the bulk density and the pseudo-particle size (-0.25 mm) ratio at charging along with the bypass return fine ratios. When the bypass return fine ratios of 0% and 15% are compared, the bulk density and the pseudo-particle size (-0.25

mm) are clearly low in the case of 15%. The bulk density and the pseudo-particle size (-0.25 mm) ratio when the bypass return fine ratios are 5 and 10% are located between the values in the cases of 0% and 15%. Although no differences are seen between the cases of 5% and 10%, it is unlikely that a specific phenomenon occurs in the bypass return fine ratios from 5 to 10%. Accordingly, it is understood that the higher the bypass return fine ratio, the lower the bulk density and the pseudo-particle size (-0.25 mm) ratio. With the increase in size of the bypass return fines, the mean bulk density and the pseudo-particle size (-0.25 mm) ratio decrease. However, no significance is seen considering fluctuations of the data in the cases.

To summarize the results, when the moisture content at charging is constant and when dry return fines are added to the granulated raw materials, the pseudo-particle size (-0.25 mm) ratio at charging decreases due to accelerated granulation because of a higher moisture content in the granulated raw materials compared to the conventional process where all raw materials are granulated at once. In addition, the bulk density decreases when the mixture contains dry particles. Whether this decrease is caused by the pseudo-particle size (-0.25 mm) ratio or increasing the friction between the wet and dry particles requires examination in the future.

2.3 Discussion

2.3.1 Factorial analysis of firing rate by adding bypass return fines

Generally, the FFS is at the bottom of a region where carbon is burning in a binder and its descending rate depends on the heat transfer from the upper zone to the lower zone in the sinter packed bed. Two types of heat transfer are considered in the sintering process. One is forced-convection heat transfer between the downward gas flow and particles. The other is conductive heat transfer directly between the particles. The former depends on the permeability of the sinter packed bed and the moisture content of the materials in it.

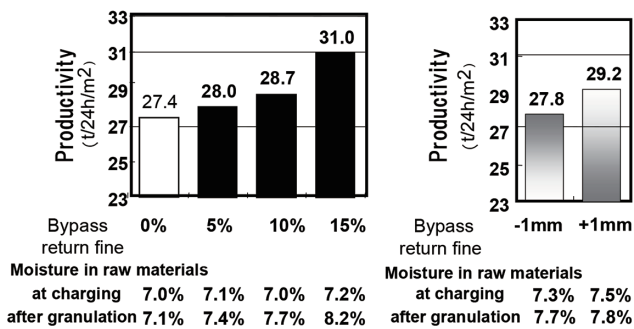


Fig. 5 Improvement of productivity by return fine addition after granulation stage

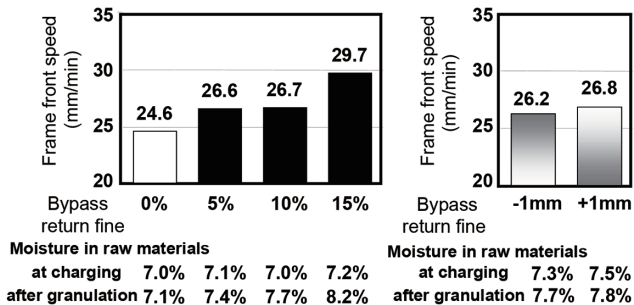


Fig. 6 Effect of return fine addition after granulation stage on frame front speed

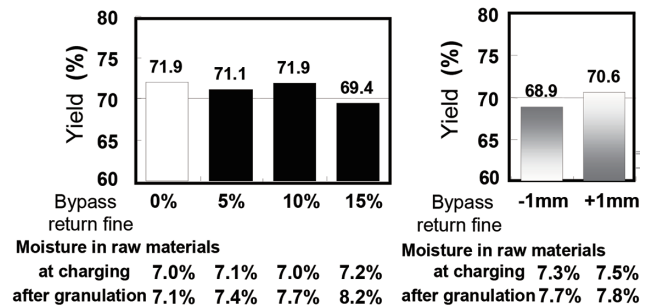


Fig. 7 Influence of return fine addition after granulation stage on yield

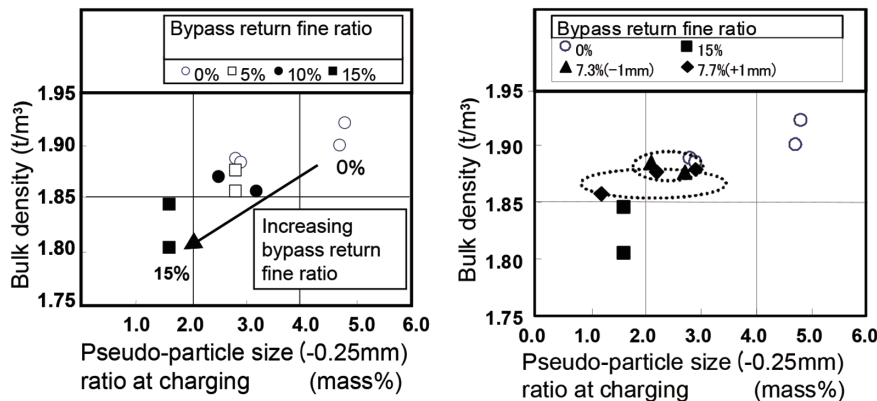


Fig. 8 Effect of return fine added after granulation stage on bulk density and pseudo-particle size at charging

The permeability of the packed bed is a function of the void ratio and the particle size as expressed by the Ergun Formula.

In fact, from Figs. 6 and 8, high FFS cases with a high bypass return fine ratio show a low bulk density and a low pseudo-particle size (-0.25 mm) ratio at charging.

The bulk density corresponds to the void ratio (ϵ) because the identical blending conditions are applied to all cases in this experiment, which means that the mean apparent density is equal. The void ratio (ϵ) is calculated by dividing the bulk density by the mean apparent density, and then subtracting the divided value from 1. The pseudo-particle size (-0.25 mm) ratio is adopted as the particle size indicating the permeability in the sintering process, because in the previous study,¹⁸⁾ a strong correlation between the pseudo-particle size (-0.25 mm) ratio and the FFS has been observed. The FFS is represented by Formula (1)

$$FFS(\text{mm/min}) = a \cdot (1 - b \cdot (d_{-0.25}(\%) / 100) \cdot (1 - c \cdot (w_{\text{charging}}(\%) / 100)) \times (\epsilon^3 / (1 - \epsilon))^{0.6} + h \quad (1)$$

$d_{-0.25}(\%)$: pseudo-particle size (-0.25 mm) ratio at charging,

$w_{\text{charging}}(\%)$: moisture content at charging, $\epsilon(-)$: void ratio.

In this Formula (1), the former term corresponding to the convection heat transfer between the gas and particles depends on the pseudo-particle size (-0.25 mm) ratio at charging, the moisture content at charging, and the void ratio (ϵ). The latter term corresponding to the conductive heat transfer directly between the particles is constant.

Based on the previous studies^{18, 19)} of examination of the FFS increase caused by the void ratio (ϵ), pseudo-particle size (-0.25 mm) ratio at charging, and moisture content at charging, the parameters (a to c and h) in Formula (1) are determined as shown in Formula (2)

$$FFS(\text{mm/min}) = 86.67(1 - 0.247(d_{-0.25}(\%) / 100) \cdot (1 - 3.20(w_{\text{charging}}(\%) / 100)) \times (\epsilon^3 / (1 - \epsilon))^{0.6} + 2.33. \quad (2)$$

In Formula (2), the pseudo-particle size (-0.25 mm) ratio at charging, moisture content at charging, and void ratio (ϵ) are limited as follows. These limitations are defined based on the experimental conditions of the previous studies^{18, 19)}

$$0.4 < d_{-0.25}(\%) < 5.6 \quad 5.3 < w_{\text{charging}}(\%) < 8.3 \quad 0.32 < \epsilon(-) < 0.42.$$

Figure 9 shows the correlation in this experiment between the FFS and the values calculated with Formula (2). The correlation factor of 0.875 is high, which proves that the formula is valid.

Based on Formula (2), the effects of the void ratio (ϵ) and the

pseudo-particle size (-0.25 mm) ratio at charging on the FFS were evaluated individually as shown in Fig. 10. The large circles in both figures are the basic points, which are determined by substituting the data of the pseudo-particle size (-0.25 mm) ratio at charging, moisture content at charging, and void ratio (ϵ) in the Formula (2) when the bypass return fine ratio is 0%. The broken lines passing the basic points are determined as the function of the void ratio (ϵ) (left figure) and pseudo-particle size (-0.25 mm) ratio at charging (right figure) with the FFS while the other parameters are constant, based on Formula (2). The solid lines are determined by the experimental results and the inclination of the solid line reflects all elements concerned for the FFS. The ratio of the inclination of the broken lines to that of the solid lines indicates a relative contribution of the void ratio (ϵ) (left figure) and the pseudo-particle size (-0.25 mm) ratio at charging (right figure) on the FFS. The effects of the void ratio and the pseudo-particle size (-0.25 mm) ratio on the FFS were evaluated as 41% and 55% relative to the total FFS increase, respectively. The added value is 96%. Accordingly, these two parameters are available for explanation.

Figure 11 shows the mechanism by which the return fines added after the granulation stage improve the productivity. When the moisture content at charging is constant, the bypass return fines can increase the moisture content in the raw materials after granulation. As shown in Fig. 4, in spite of the small amount of particles (-0.25 mm) contained in the bypass return fine, the pseudo-particle size (-0.25 mm) ratio at charging in the sinter plant decreases with the increase in the bypass return fine ratio. The reason is that a higher

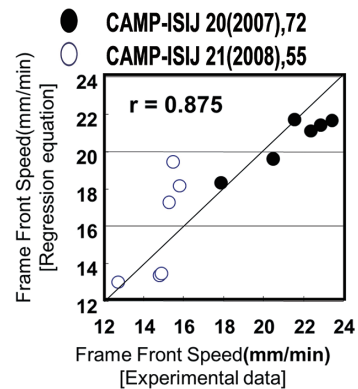


Fig. 9 Verification of regression equation

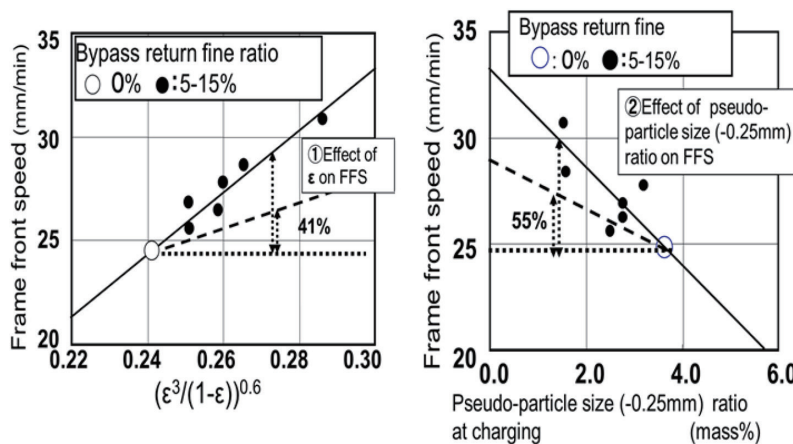


Fig. 10 Effect of void ratio and pseudo-particle size at charging on flame front speed at return fine addition after granulation stage

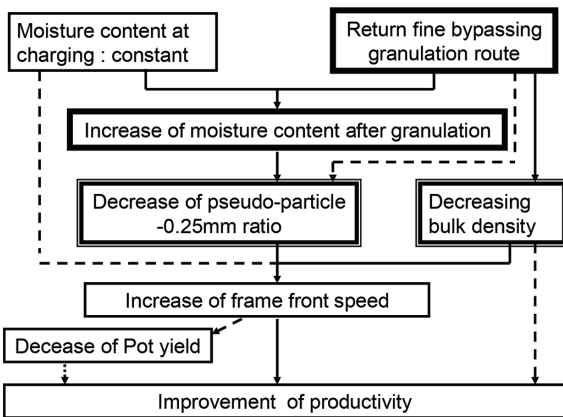


Fig. 11 Effect of RF-MEBIOS (return fine bypassing granulation route) on improvement of productivity

moisture content in the granulated raw material accelerates the granulation and this surpasses the increase of the ungranulated return fine (-0.25 mm) ratio. In addition, the bulk density decreases by adding dry return fines to the granulated wet material.

Both decreases in the pseudo-particle size (-0.25 mm) ratio at charging and the bulk density contribute to the increase of the FFS. The effects of the decrease in the yield due to the increased FFS and the direct decrease of the product sintered ore due to the decreased bulk density at charging were minor compared to the FFS increase, so the productivity was improved.

2.3.2 The mechanism of decreasing bulk density

Sato et al.²⁰⁾ have reported the function of the moisture content in the sinter raw material pretreatment process in which as the moisture content increases, pseudo-particles grow in granulation. However, an excess moisture content fills the voids between the pseudo-particles in the sinter packed bed in the pretreatment process and thereby the moisture content hinders the ventilation unlike the case of granulation. In addition, Kawaguchi et al.¹⁹⁾ have reported the formation of sinter packed beds and that the moisture content value with the maximum permeability is low in the case of charging from a higher point. These facts indicate that the RF-MEBIOS process may function to suppress the decrease in voids in packed beds due to high moisture content granulation and charging by drop. Thus, adding dry particles after granulation forms a composite bed consisting of granulated wet particles and ungranulated dry particles. This composite bed may enhance the resistance to shock from drop (charge). To verify this, the shear strength of packed beds was examined and studied in an all-around shearing test.

Figure 12 outlines the all-round shearing test. For samples, 76.4 dry-g pisolite ore (4.7% initial moisture content) and 20.0 dry-g return fines (0% initial moisture content) were prepared. Then, they were crushed to -0.25 mm in advance. As the procedures, the 76.4 dry-g pisolite ore and water were mixed such that the moisture content after the granulation was approximately 14.0%. Then, 20.0 dry-g of return fines were added and lightly mixed such that the moisture content in the composite bed at charging was 11.1%. The samples were charged to a shearing cell in which the upper section was fixed and the lower section was movable, with a diameter of 60 mm. It was sheared at a constant rate of approximately 3.0 mm/min while designated perpendicular stress was applied. The shear strength was measured based on the load in the shear plane direction. The perpendicular stress was applied to three points (49, 98, and 147 kPa) for each sample. Finally, the internal friction coefficient and adhe-

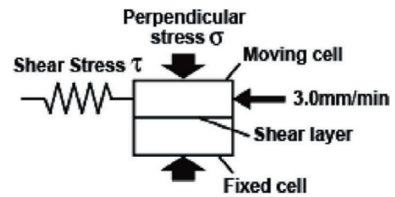


Fig. 12 Experimental procedures of shear test

Table 2 Experimental conditions of shear test

	Base		RF-MEBIOS
Iron ore (dry-g)	76.4	76.4	76.4
Dry particle (dry-g)	20.0	20.0	0.0
Moisture after granulation (%)	3.7	11.1	14.0
Dry particle (add) (dry-g)	0.0	0.0	20.0
Moisture at charging (%)	3.7	11.1	11.1

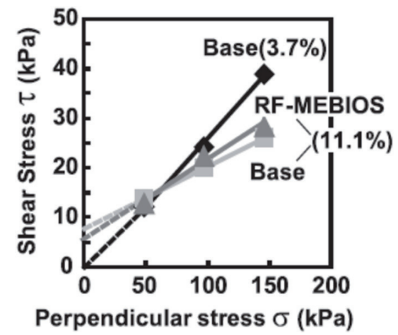


Fig. 13 Decrease of friction coefficient by RF-MEBIOS

sion of the materials were calculated by Mohr-coulomb yield criterion²¹⁾ Formula (3).

Other samples were prepared by mixing iron ore and return fines without adding water (3.7% moisture content at charging) and by mixing iron ore, return fines, and water at once (11.1% moisture content at charging). Each sample was subjected to a shear test and the base and composite bed (RF-MEBIOS process) were compared (Table 2).

$$\tau = \sigma \tan\phi + C \tag{3}$$

τ : shear stress (kPa), σ : perpendicular stress (kPa)

ϕ : internal frictional angle (°)

$\tan\phi$: internal friction coefficient (-), C : adhesion (kPa)

Figure 13 shows the shear test results. The horizontal axis is the perpendicular stress and the vertical axis is the measured shear strength. In the figure, the tilt of the lines connecting the measured values indicates the internal friction coefficient and the y-intercept indicates the adhesion, as expressed by Formula (3). Comparing the bases of (3.7%) and (11.1%), when the influence of the moisture difference is compared under the same raw material blending condition, the lower the moisture content, the higher the internal friction coefficient. Then, the base (11.1%) and the RF-MEBIOS (11.1%) were compared; the case where all the materials were mixed at a time as conventionally performed was compared to the case where some raw materials were added in the later process to form a compound consisting of dry particles and wet particles. It is confirmed that forming a compound obtains a higher internal friction coefficient even if the blending and the total moisture content are the same (Table 3).

Table 3 Experimental results of shear test

Case (moisture content)	$\tan\phi$: Friction coefficient	C: Adhesion
Base (3.7%)	0.274	0.0
Base (11.1%)	0.124	7.8
RF-MEBIOS (11.1%)	0.159	5.8

Terashita et al.²²⁾ performed all-round shear tests of various types of powder and granular materials at constant capacity and load to examine the influence of the moisture content on the internal friction coefficient. They have reported that the internal friction coefficient of the powder and granular materials is the highest when the moisture content is 0% and it decreases in the pendular area as the moisture content increases. It is almost constant from the funicular area to the early stage of the capillary area and it decreases again in the following capillary to slurry areas. Therefore, a higher friction of RF-MEBIOS is caused by the existence of dry particles, which has a high internal friction coefficient, in the raw materials at charging.

In addition, when the shear strength shown in Fig. 13 is regarded as the deformation resistance of the powder and granular materials, the resistance of the base and RF-MEBIOS process reverses with a certain perpendicular stress as the boundary. When the perpendicular stress is hardly applied, the deformation resistance of the base is higher. When the perpendicular stress is applied to some extent, the deformation resistance of the RF-MEBIOS process is higher.

In the sinter process, granulated materials taken out by a roll feeder are charged into a pallet by dropping from a chute. In this experiment, a packed bed is formed on the raw material charged by dropping. At this time, the raw material receives various types of force such as force when the inertia movement of each pseudo-particle collide with each other and force when the weight of the raw material flowing down and drop impact spread to the area that already has a packed bed. The raw material, the side of which is fixed to the container outer wall, receives the vertical force. It is considered that the material receives shear force in a packed state like turn-

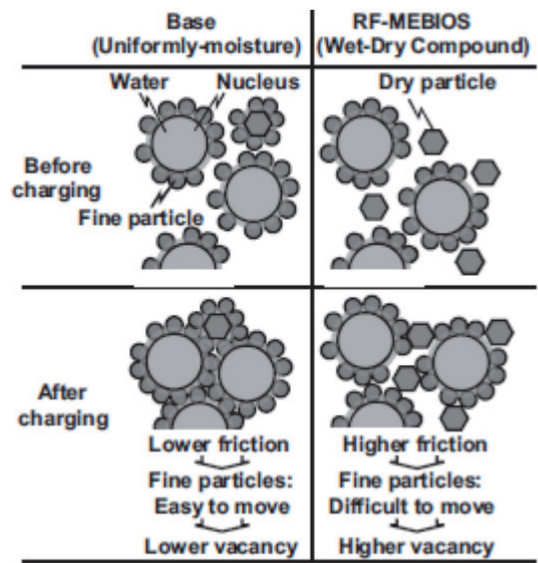


Fig. 14 Increasing vacancy of packed bed by RF-MEBIOS

ing the sample in Fig. 12 by 90 degrees. The higher void ratio in the RF-MEBIOS process is caused by a higher internal friction coefficient of the packed bed functions as the resistance to the force of drop impact and downward load, and consequently, the vacancy becomes easy to maintain in RF-MEBIOS as illustrated in Fig. 14. A future task is to analyze which force a raw material receives and to what extent when a packed bed is formed.

3. Practical Application to a Commercial Plant

3.1 Application to Kashima sinter plant No.3

3.1.1 Layout of return fine transportation

Figure 15 illustrates the material flow at the practical sinter plant. Transportation of return fines diverges into two routes by a divergence damper. One is to the existing return fine bin and the other

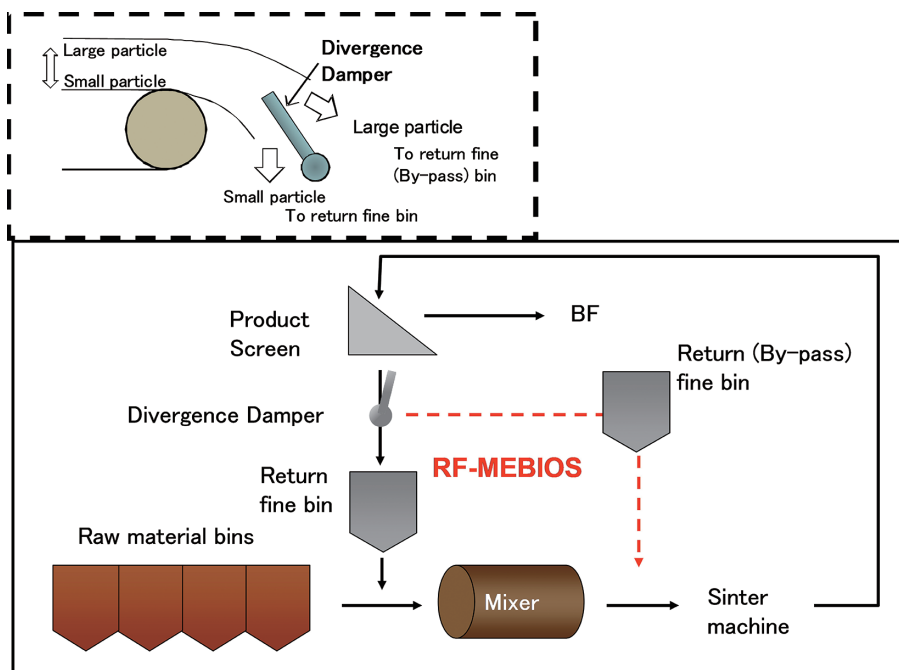


Fig. 15 Layout of return fine transporting route at commercial sinter plant

to the new bypass return fine bin.

The return fines from the existing return fine bin and the other sinter raw materials are mixed and granulated together with water in the mixer. The return fines from the bypass return fine bin are added after the mixer. The section enclosed in broken lines in Fig. 15 shows the positional relationship between the damper and belt conveyor. The damper position is adjusted to control the ratio of the bypass return fines. The damper can separate the return fines between the upper layer (bypass return fines) and the lower layer (granulation return fines). The belt conveyor discharges course particles as the upper layer, so relatively large particles are transported to the bypass return fine bin.

This divergence method was adopted because of the results of the pot test, in which large particles bypassing the mixer are effective for the FFS and the productivity as compared with bypassing small particles. Figure 16 shows the pseudo-particle size (-0.25 mm) ratios for the bypass return fines and total return fines at each bypass return fine ratio. The ratio for the bypass return fine is lower than that of the total return fines. With the increase of the ratio of the bypass return fines, the pseudo-particle size (-0.25 mm) ratio of the bypass return fines becomes closer to that of the total return fines.

In the practical plant test, the ratios of the bypass return fines to the sinter mixture were 20%, 14%, and 8% with the constant moisture content (6.4–6.5%) at charging. As shown in Fig. 15, at the high bypass return fine ratio (to the total mixture), the moisture content (%) after the granulation is high. It is 7.9%, 7.5%, or 7.1% in each case.

3.1.2 Operational results

The operational results are shown in Fig. 17. A high ratio of the bypass return fines (20% to the total sinter mixture) increases the productivity (> 620 t/h) due to high FFS. The productivity improvement may be caused by the increased pseudo-particle size as is the case with the sinter pot test in the previous chapter.

Figure 18 shows the effect of the moisture content after granulation on GI (-0.25 mm), GI (-0.25 mm) is defined by Formula (3). The index means the granulating ratio for particles with a diameter of 0.25 mm or smaller. A (-0.25 mm) and B (-0.25 mm) correspond to real particles and pseudo-particles, respectively. B (-0.25 mm) was measured by sieving for 15 s without tapping after drying for 2 h under 105 degrees C. Thereafter, all the sieved samples were collected and A (-0.25 mm) was measured by sieving for 5 min with tapping. These analyses were performed for both raw materials after the granulation and at charging to calculate GI (-0.25 mm) for each

$$GI(-0.25\text{mm})(\text{mass}\%) = \left(1 - \frac{B(-0.25\text{mm})}{A(-0.25\text{mm})}\right) \times 100 \quad (4)$$

A(-0.25 mm): -0.25 mm ratio of real particle (mass%)

B(-0.25 mm): -0.25 mm ratio of pseudo-particle (mass%).

Figure 18 confirms that the GI (-0.25 mm) is high at a high moisture content after the granulation. The relation between the moisture content after the granulation and GI (-0.25 mm) is represented by the quadratic formula shown in Fig. 18.

Figure 19 shows the effect of the bypass return fine ratio on the GI (-0.25 mm) of the raw material after the granulation and at charging. The GI (-0.25 mm) after the granulation is high at a high ratio of the bypass return fine due to a high moisture content (%) after the granulation. The GI (-0.25 mm) of the raw materials at charging decreases due to the addition of the bypass return fines containing small particles as compared to the GI (-0.25 mm) of the pseudo-particles after the granulation. However, the GI (-0.25 mm) of the pseudo-particles at charging remains higher in the case of the high bypass return fine ratio even with the effect of such decrease. It

Moisture condition in each condition			
Bypass return fine ratio (mass%)	20	14	8
Moisture content after granulation (mass%)	7.9	7.5	7.1
Moisture content at charging (mass%)	6.4	6.5	6.5

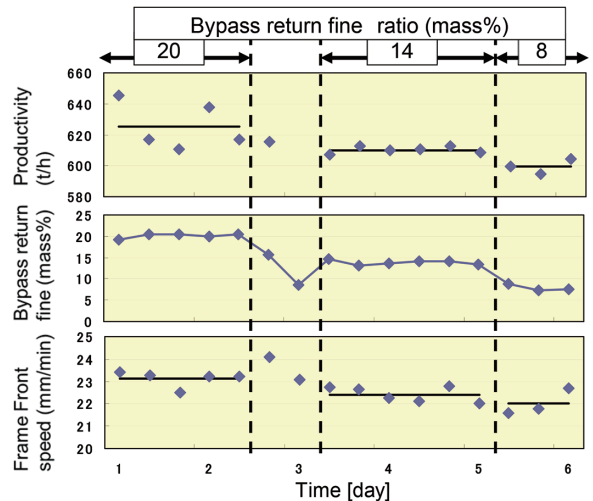


Fig. 17 Operational performances at varying bypass return fine ratio

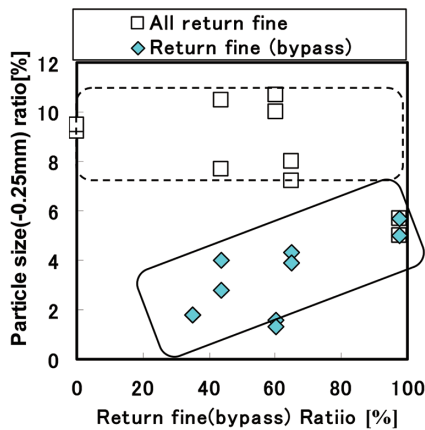


Fig. 16 Influence of bypass return fine ratio on particle size

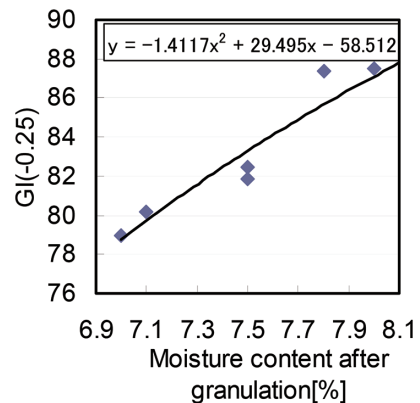


Fig. 18 Increasing GI(-0.25 mm) by high moisture content after granulation

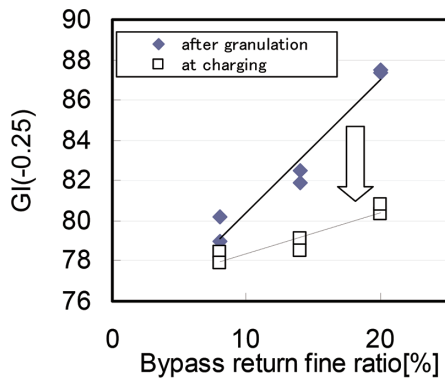


Fig. 19 Effect of bypass return fine ratio on GI(-0.25mm)

suggests that the granulation with a high moisture content is affected more than that of adding small particles contained in the ungranulated bypass return fines. The results match the pot test results qualitatively.

An optimum bypass return fine ratio is a key parameter for sinter plant operation. To this end, the relation between the bypass return fine ratio and the small particle (-0.25 mm) ratio in pseudo-particles at charging was evaluated by the procedures below. The premise conditions are as follows.

- -0.25-mm particle ratio in the sinter raw materials except the return fines: 25%
- Return fine ratio to the total sinter mixture: 20%
- -0.25-mm particle ratio in the return fines: 4.4%
- Moisture content at charging: 7.0%

The quantity of -0.25-mm particles in the sinter raw material at charging is considered to be the sum of -0.25-mm particles in the bypass return fines and those in the granulated raw materials because the bypass return fines charged into the sinter plant are not granulated. This is represented as follows:

$$\begin{aligned}
 & \text{-0.25-mm particle ratio in the sinter mixture at charging (\%)} \\
 & \quad \times \text{Sinter mixture weight at charging (t/h)} \\
 = & \text{-0.25-mm particle ratio in the granulated raw material (\%)} \\
 & \quad \times (\text{Sinter mixture weight (t/h)} - \text{Bypass return fine weight (t/h)}) \\
 + & \text{-0.25-mm particle ratio in the bypass return fine (\%)} \\
 & \quad \times \text{Bypass return fine weight (t/h)}. \tag{5}
 \end{aligned}$$

For the calculation of Formula (5), sinter mixture weight at charging (t/h) and bypass return fine weight (t/h) are given as operational parameters. A particle ratio of -0.25 mm in the bypass return fines (%) is defined in Fig. 13. The -0.25-mm particle ratio in the granulated raw materials is calculated from the GI (-0.25 mm) and -0.25-mm particle ratio in the raw materials before the granulation, based on Formula (3). The GI (-0.25 mm) is calculated by the regression formula in Fig. 18. The -0.25-mm particle ratio in the raw materials before the granulation is calculated from the aforementioned three parameters: -0.25-mm particle ratio in the sinter raw materials except the bypass return fines (25%), -0.25-mm particle ratio in the return fines (4.4%), and the granulation return fine ratio.

Figure 20 shows the relation between the bypass return fine ratio (to the total sinter mixture), GI (-0.25 mm), and the moisture content after the granulation. Figure 21 shows the influence of the bypass return fine ratio (to the total sinter mixture) on the pseudo-particle size (-0.25 mm) ratios before and after the granulation using the GI (-0.25 mm) shown in Fig. 17. With the increase of the bypass return fine ratio, the pseudo-particle size (-0.25 mm) ratio after the granulation decreases, in spite of the increased pseudo-par-

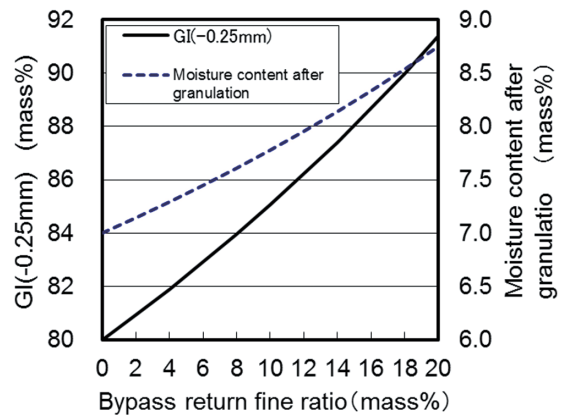


Fig. 20 GI(-0.25 mm) and moisture content after granulation corresponding to bypass return fine ratio

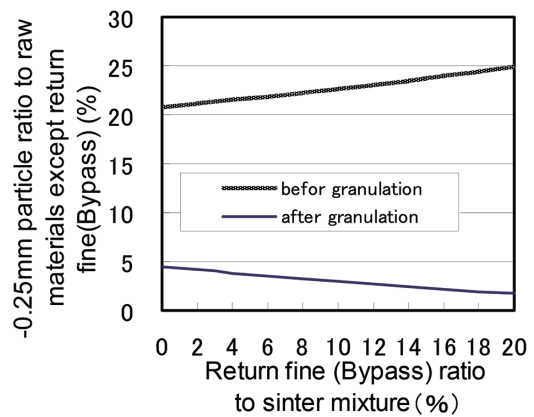


Fig. 21 Influence of bypass return fine ratio on particle size (-0.25 mm) ratio before and after granulation

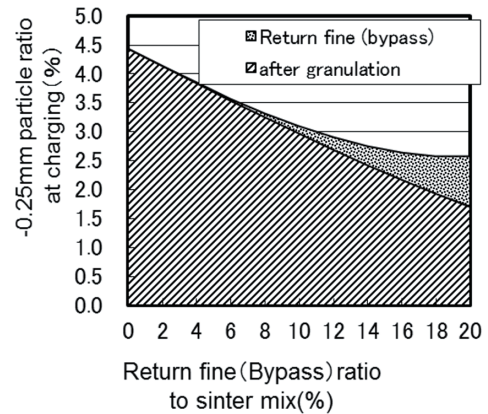


Fig. 22 Influence of bypass return fine ratio on pseudo-particle size (-0.25 mm) ratio at charging

ticle size (-0.25 mm) ratio before the granulation.

Figure 22 shows the influence of the bypass return fine ratio on the pseudo-particle size (-0.25 mm) ratio at charging, distinguishing between the pseudo-particle size (-0.25 mm) ratio in the sinter mixture at charging and the pseudo-particle size (-0.25 mm) ratio in the granulated raw materials. The ratio originated from the granulated raw material is the pseudo-particle size (-0.25 mm) ratio in the granulated raw material shown in Fig. 21. The results in Fig. 22

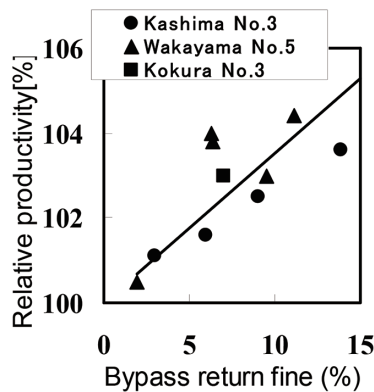


Fig. 23 Universal effect of RF-MEBIOS on productivity

show that under the conditions assuming the test using sinter plant No.3 of the practical plant, the optimum bypass return fine ratio is 18% (to the total sinter mixture).

3.2 Productivity improvement at practical plants

RF-MEBIOS, which is a technique of return fine bypassing granulation, was applied to three sinter plants at former Sumitomo Metal Industries, Ltd. before its consolidation to improve the productivity, as shown in Fig. 23. After the consolidation, the RF-MEBIOS process was introduced to Kimitsu and Yawata Works and the applied plants are under operation.

4. Conclusions

High permeability of sinter packed beds for sinter productivity improvement has been achieved by the Return Fine - Mosaic Embedding Iron Ore Sintering (RF-MEBIOS) process, in which dry ungranulated return fines are added to granulated wet raw materials.

The permeability is increased by two factors of a low fine pseudo-particle size (~ 0.25 mm) ratio and a low bulk density. The former is caused by granulation with a high moisture content due to the addition of dry return fines after the granulation when the moisture content at charging is constant.

This process was applied to four steelworks of Nippon Steel Corporation and all plants have produced improved productivity.

References

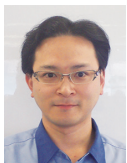
- 1) Sawamura, J., Itou, K., Uno, N., Oomizu, M.: Tetsu-to-Hagané. S416, 61 (1975)
- 2) Nakajima, R., Komatsu, S., Shimizu, M., Inoue, H., Takagi, A.: Tetsu-to-Hagané. S765, 61 (1987)
- 3) Kawaguchi, T., Kuriyama, K., Sato, S., Takada, K.: Tetsu-to-Hagané. 1924, 73 (1987)
- 4) Kawaguchi, T., Kuriyama, K., Sato, S., Takada, K.: Tetsu-to-Hagané. 1642, 76 (1990)
- 5) Haga, T., Ohshio, A., Hida, Y., Fukuda, H., Ogata, N.: Tetsu-to-Hagané. 233, 83 (1997)
- 6) Matsumura, T., Miyagawa, K., Yamagata, Y.: ISIJ International. 485, 45 (2005)
- 7) Kasai, E., Shu, I., Kobayashi, S., Omori, Y.: Tetsu-to-Hagané. 520, 70 (1984)
- 8) Suzuki, S., Sato, K., Fujimoto, M.: Tetsu-to-Hagané. 1932, 73 (1987)
- 9) Tashiro, K., Soma, H., Hosotani, Y., Konno, N.: Tetsu-to-Hagané. S24, 63 (1977)
- 10) Wajima, M., Hosotani, Y., Shibata, J., Soma, H., Tashiro, K.: Tetsu-to-Hagané. 1719, 68 (1982)
- 11) Hida, Y., Itoh, K., Sasaki, M.: Tetsu-to-Hagané. S82, 66 (1980)
- 12) Kawaguchi, T.: CAMP-ISIJ. 129, 5 (1992)
- 13) Kamijo, C., Matsumura, M., Kawaguchi, T.: CAMP-ISIJ. 120, 17 (2004)
- 14) Kawaguchi, T., Kamijo, C., Matsumura, M.: Tetsu-to-Hagané. 779, 92 (2006)
- 15) Kawaguchi, T., Usui, T.: ISIJ International. 414, 45 (2005)
- 16) Kasai, E., Komarov, S., Nushiro, K., Nakano, M.: ISIJ International. 538, 45 (2005)
- 17) Kamijo, C., Matsumura, M., Kawaguchi, T.: ISIJ International. 544, 45 (2005)
- 18) Matsumura, M., Kawaguchi, T.: CAMP-ISIJ. 72, 20 (2007)
- 19) Kawaguchi, T., Matsumura, M.: CAMP-ISIJ. 55, 21 (2008), CD-ROM
- 20) Sato, S., Yoshinaga, M., Ichidate, M., Kawaguchi, T.: Tetsu-to-Hagané. 2174, 68 (1982)
- 21) Edited by Kawakami, F.: Soil Engineering Practice-Basics. Morikita Publishing Co., Ltd.
- 22) Terashita, K., Miyanami, K., Okajima, M., Furubayashi, K.: Journal of the Society of Powder Technology (in Japanese). 18 (9), 657-665 (1981)



Masaru MATSUMURA
Chief Researcher, Ph.D.(Environmental studies)
Ironmaking Research Lab.
Process Research Laboratories
20-1 Shintomi, Futtsu City, Chiba Pref. 293-8511



Chikashi KAMIJO
Senior Manager, Ph.D.(Engineering)
Experimental Blast Furnace Project Div.
Process Research Laboratories



Yasuhide YAMAGUCHI
Senior Researcher
Ironmaking Research Lab.
Process Research Laboratories